Author's Accepted Manuscript

www.elsevier.com/locate/dsr2

Modification of deep waters in Marguerite Bay, western Antarctic Peninsula, caused by topographic overflows

Hugh J. Venables, Michael P. Meredith, J. Alexander Brearley

PII: S0967-0645(16)30284-3
DOI: http://dx.doi.org/10.1016/j.dsr2.2016.09.005
Reference: DSRII4137

To appear in: *Deep-Sea Research Part II*

Received date: 25 February 2016
Revised date: 26 September 2016
Accepted date: 28 September 2016

Cite this article as: Hugh J. Venables, Michael P. Meredith and J. Alexander Brearley, Modification of deep waters in Marguerite Bay, western Antarctic Peninsula, caused by topographic overflows, *Deep-Sea Research Part II* http://dx.doi.org/10.1016/j.dsr2.2016.09.005

Modification of deep waters in Marguerite Bay, western Antarctic Peninsula, caused by topographic overflows

Hugh J. Venables, Michael P. Meredith, J. Alexander Brearley

British Antarctic Survey, Cambridge, U.K.

Abstract

Circumpolar Deep Water (CDW) intrudes from the mid-layers of the Antarctic Circumpolar Current onto the shelf of the western Antarctic Peninsula, providing a source of heat and nutrients to the regional ocean. It is well known that CDW is modified as it flows across the shelf, but the mechanisms responsible for this are not fully known. Here, data from underwater gliders with high spatial resolution are used to demonstrate the importance of detailed bathymetry in inducing multiple local mixing events. Clear evidence for overflows is observed in the glider data as water flows along a deep channel with multiple transverse ridges. The ridges block the densest waters, with overflowing water descending several hundred metres to fill subsequent basins. This vertical flow leads to entrainment of overlying colder and fresher water in localised mixing events. Initially this process leads to an increase in bottom temperatures due to the temperature maximum waters descending to greater depths. After several ridges, however, the mixing is sufficient to remove the temperature maximum completely and the entrainment of colder thermocline waters to depth reduces the bottom temperature, to approximately the same as in the source region of Marguerite Trough. Similarly, it is shown that deep waters of Palmer Deep are warmer than at the same depth at the shelf break. The exact details of the transformations observed are heavily dependent on the local bathymetry and water column structure, but glacially-carved troughs and shallow sills are a common feature of the bathymetry of polar shelves, and these types of processes may be a factor in determining the hydrographic conditions close to the coast across a wider area.

Keywords: West Antarctic Peninsula; Deep water modification; Ocean Gliders; Time Series; Antarctica

1 Introduction

The flow of Circumpolar Deep Water (CDW) onto and across the continental shelf along the western Antarctic Peninsula (WAP) is key to understanding the heat flux reaching floating ice sheets and glaciers. This water mass originates in the mid-layers of the Antarctic Circumpolar Current (ACC), the southernmost parts of which lie adjacent to the continental slope in the vicinity of the WAP. Having intruded onto the shelf, a modified version of CDW is created (mCDW) through a combination of mixing, heat loss to the atmosphere (Turner *et al.*, 2013) and ice formation and melt, with each process having different spatial and temporal patterns (Martinson *et al.*, 2008). Satellite measurements show that the WAP glaciers are generally thinning rapidly (Pritchard *et al.*, 2009), concurrent with a retreat in most valley glaciers along the Peninsula (Cook *et al.*, 2005), with both processes contributing to global sea level rise. Despite recent warming (Turner *et al.*, 2005), atmospheric-driven melting and iceberg calving appear insufficient to explain the rates of melt observed, while the heat content in mCDW suggests a likely source of the energy, however sufficiently accurate estimates of ocean heat flux in the area are presently lacking (Pritchard *et al.*, 2012; Rignot *et al.*, 2013) though a warming trend has been observed in this water mass (Schmidtko *et al.*, 2014).

Several mechanisms have been proposed for the flow of CDW onto the shelf, involving crossing the physical and dynamical barrier of the steep shelf break. These include direct flow into canyon mouths, eddy shedding, flow-topography interactions where the shelf-break curves strongly and Ekman induced upwelling (Klinck and Dinniman, 2010; Martinson and McKee, 2012; Moffat *et al.*, 2009). Deep canyons that dissect the WAP shelf are filled with mCDW and, due to their enclosed basins have slow currents. Above this deep layer, the circulation is less constrained by bathymetry and is complex and time-varying, though there have been indications of a system of gyres separating the northeastward flow at the shelf-break from a general southward flow close to land. This latter circulation feature is associated with seasonal wind forcing and density gradients associated with enhanced freshwater inputs (Moffat *et al.*, 2008). Consideration of isotopic tracer data has revealed that these freshwater inputs are predominantly from meteoric sources (glacial melt and precipitation) (Meredith *et al.*, 2013)

As well as glacial ice, there have also been considerable changes to sea ice in Antarctica. A small but significant circumpolar increase in sea ice is the result of large, counteracting regional gains and losses (Holland and Kwok, 2012). For the WAP shelf, the sea-ice season has shortened considerably (Stammerjohn *et al.*, 2008a) such that the sea surface is exposed to the atmosphere for longer. Significant changes are seen in the winter mixed-layer depth and summer stratification, heat uptake and seasonal thermocline depth in the Rothera Time Series (RATS) following variations in winter sea-ice cover (Venables and Meredith, 2014), demonstrating the sensitivity of the ocean structure to such climatic changes.

The bathymetry in Marguerite Bay is the result of erosion and deposition during glacial periods when sea levels were lower and the Antarctic continental ice field more extensive (Livingstone *et al.*, 2013). Marguerite Trough is an important bathymetric feature, providing a route for CDW to flow onto the shelf and into Marguerite Bay (Klinck *et al.*, 2004). Another feature of the glacial geomorphology on the shelf is the presence of overdeepened depressions with shallow sills. These present a barrier to flow across the shelf, potentially making the cross-shelf flow sensitive to shoaling of isotherms or changes to sea level.

The focus of this study is flow/bathymetry interactions over sills and within enclosed topographic depressions, which we show to be important in causing water mass modification. We identify key locations where significant vertical flows and mixing occurs, which are important in determining how mCDW escapes the deep troughs and interacts with the bathymetry and overlying waters. We also present data for enclosed depressions south of Adelaide Island where the shallow sills lead to cold bottom temperatures and Palmer Deep, which is warmer at depth than other locations along the shelf. We use high-resolution hydrographic data collected by autonomous Slocum gliders over three seasons together with hydrographic data from a short research cruise and data from an oceanographic/biogeochemical time series conducted close to Rothera Research Station in northern Marguerite Bay.

2 Methods and data

Data were collected using deep (1000 m rated) Slocum ocean gliders. These were instrumented with a pumped CTD (Conductivity, Temperature, Depth) unit, plus sensors for chlorophyll and turbidity. The glider altimeters allowed sampling to within 20 m of the seabed through the deployments. Data used here are from gliders deployed and recovered at the British Antarctic Survey base at Rothera in the 2012/13 and 2013/14 seasons, and a third launched from the RRS *James Clark Ross* in the 2015/16 season in transit to Rothera, which was flown to the United States' Palmer Station (Fig. 1). At the time of writing, only low-resolution data transmitted over Iridium satellite are available from this latter glider.

The temperature and salinity values from the Rothera-launched gliders were compared against a concurrent cast in Ryder Bay collected using an SBE19 CTD as part of the Rothera Oceanographic Time Series (RATS). The glider profiles extend deeper than 400 m, beyond than the 350 m deep sill that separates Ryder Bay from the ocean beyond, thus ensuring stability of the deep water mass used for intercomparison purposes. Although slight differences (≈0.01°C and 0.001 in salinity) were detected, there was no drift on any deployment and no adjustments have been made.

The RATS instruments are rotated for servicing and calibration every two seasons, and data are compared against the ARSV *Laurence M. Gould*'s SBE911 CTD each summer on casts taken inside and outside Ryder Bay. During these comparisons, the RATS CTD(s) are fixed to the larger frame on the ARSV *Laurence M. Gould*, one metre above the ship's instruments. This, together with weekly collection of discrete salinity samples for calibration purposes, leads to a series of time-dependent calibrations for each instrument's duration at Rothera (Clarke *et al.*, 2008; Venables *et al.*, 2013) as well as joint casts between the two RATS CTDs in summers when they are swapped round, further ensuring consistency through the time series.

The gliders deployed from Rothera occupied their sections twice, once on the outbound journey from the base, and once on their return, and extremely good agreement was found between the two legs.To investigate possibly hysteresis, glider data were compared between upward and subsequent downward dives while the vehicles held station. There was a very slight systematic offset between up and down casts, matching changing gradients in the temperature profile, peaking at $3x10^{-3}$ °C, or about 10cm offset on each of the profiles. As this effect is small compared with the natural variability caused by e.g. internal waves (±0.3 °C) and to the effects studied, both up and down casts are used here, with no correction applied.

A follow-up cruise, designated JR307, was undertaken to the enclosed depressions south of Adelaide Island between 31 December 2014 and 7 January 2015. This involved CTD casts, water samples for biogeochemical measurements, and benthic biology sampling inside and outside of the cold holes (Fig. 2). The physical data are presented here, using calibrations obtained during a CTD transect across Drake Passage immediately afterwards (King and Firing, 2015).

Bathymetry data used were the 15-second resolution Southern Ocean Global Ocean Ecosystems Dynamics (SO GLOBEC) compilation (Bolmer *et al.*, 2004) and, for Palmer Deep area, the International Bathymetric Chart of the Southern Ocean (IBCSO) version 1.0 (Arndt *et al.*, 2013).

3 Results

3.1 Bathymetric setting

The main glider track from Jan/Feb 2014 follows a channel linking Marguerite Trough and Laubeuf Fjord, the deep trough that feeds into Ryder Bay (Fig. 1). This channel is the only deep connection between the troughs. Swath bathymetry maps show a series of transverse ridges across the channel. As detailed below, the deep water flows from Marguerite Trough to Laubeuf Fjord and the ridges block the densest water and lead to localised mixing between mCDW and overflowing water. There are no other deep routes connecting Laubeuf Fjord with Marguerite Trough so the return flow must be at shallower depths. This pattern of overdeepened depressions and sills is common across the WAP shelf due to its glacial history and a similar pattern is found near Anvers Island. The details are inevitably different in each location but the processes described are repeatable across a wide area.

3.2 Blocking and overflows

It is evident from the salinity profiles (Fig. 3d) that the densest waters are blocked by the ridge (note that in the temperature and depth range of this study, salinity is the dominant control on density, hence only salinity is shown, with density profiles looking almost identical in form). There is a step change in near-bottom salinity of 0.005 after the first ridge (Fig. 3a). The downstream cavity must therefore be filled by water from shallower depths that overflow the sill, and which subsequently descend by 300-500 m. This process is repeated at several ridges along the length of the channel, each time creating a step change in deep salinity. The overall reduction in salinity is approximately 0.06 by the end of the section.

Initially the water column has a well-structured temperature profile typical of the Southern Ocean, with a temperature maximum >1.4 °C at 300-400 m with temperatures reducing slightly with depth to the bottom, and reducing rapidly at shallower depths to a temperature minimum comprising Winter Water (WW), the remnant of the upper-ocean winter mixed layer (Fig. 3c, 4b). After the first two ridges the near-bottom temperature increases by 0.05 °C. This can only happen by a downward flow of water from close to the temperature maximum as water flows over a sill into the basin. Lateral advection of warmer waters is not possible within a confined basin and there is no source water at that depth that is warm enough. An endmember analysis of temperature and salinity together shows that the downstream profiles in each case can only be created if the deepest waters (200-300 m) are excluded. Although a temperature maximum still exists subsequent to this first downward flow, it is less well defined than upstream of the ridge.

There are further changes after each subsequent crossing of a sill. The effect of each is to entrain cold thermocline water into the deep water, causing the bottom temperatures to decline once the overlying temperature maximum is eroded away. By Laubeuf Fjord this results in bottom temperatures being approximately equal to their values in Marguerite Bay. Comparison of temperature data from Marguerite Trough with that from Laubeuf Fjord shows the largest change at 350 m and then reducing with depth, whereas the salinity profiles show the greatest change at the seabed.

Detailed evidence of dense overflows can be seen in data collected in 2012 when the glider held station close to the inflow to Laubeuf Fjord (67° 55’S, 68° 25’W) for a week. It is evident in the profiles that properties down to 620 m (100 m below the sill depth) are consistent whereas in the bottom 100 m there is greater variability, with some profiles showing a strong increase in salinity near the bottom. In an enclosed depression this is clear evidence of a downward flow as any mixing processes would lead to most variability close to the sill depth and a reduction with depth rather than an increase. Similar structures are seen in other areas downstream of sills.

3.4. Density and temperature sections

The effects of the overflows on the isopycnal depths can be seen in Fig. 4a, with the isopycnals deepening in steps or stopping completely at each sill, matching the loss of the temperature maximum (Fig. 4b). There is a clear sequential process along the channel, with the water properties changing a small amount at each sill but with isopycnal depths deepening by over 100 m. Overall, this leads to larger changes observed with less dense deep water and an erosion of the temperature structure.

3.3 Evidence of enhanced mixing

The flows of water down into the enclosed depressions must clearly be matched by an upwards movement out of the basin. In the short term this may be due to displacement of less dense water when there is an increase in density of the source water. Vertical mixing will reduce the density within the depressions leading to further overflows, modulated by natural variability in the density of the source waters at the sill depth. As shown above, with each overflow there is entrainment of overlying waters. This mixing leads to a straightening of the θ/S curves (Fig. 3b), with a reduction in temperature at S>34.53 and an increase at lower salinities. This 'pivot' salinity is found at about 200 m, well above all the sill depths. The structure of the temperature maximum is straightened, becoming a linear θ/S relationship, indicative that significant mixing has occurred. At lower salinities, there is an increase in the corresponding temperature. This indicates the exchange between these cold thermocline waters and the warmer waters below as they overflow the ridges. As well as the overflow processes, there will be a range of other mixing processes occurring due to the complicated bathymetry and proximity of shallow areas.

3.5 Temperature and salinity on isopycnals

Due to the high spatial density of profiles collected by the glider, it is possible to derive information from the hydrographic data concerning where mixing has happened. This can be done by considering changes in temperature and salinity along isopycnals, and the variance of these properties. This approach is suitable for the present application as the route of the deep water is known from the changes in the near-bottom temperature and salinity. At depth, these changes occur as steps, linked to large changes in the depth of some isopycnals (Fig. 3d,4a), whereas at shallower depths the flow through a narrow channel will also very likely enhance the background level of mixing. The data presented are for the return leg along the channel, the outward leg shows a very similar pattern.

The bulk properties show notable changes along isopycnals (Fig. 5). There is a reduction in temperature in the densest layers; this is necessarily matched by a freshening and the reverse pattern at density levels shallower than 220 m. This pattern is largely coherent through the water column below about 150 m and supports the suggestion from the θ/S plots that the shallow changes are linked to processes induced by the deep bathymetry, even though these depths are sufficiently shallow that the flow is not necessarily controlled by the bathymetry directly. Surface variability will be introduced in winter due to varying levels of ice cover and surface mixing by winds and brine rejection.

The variance of properties along isopycnals also reduces strongly with distance in the onshore direction. Profiles have been split into three sections, separated by the red sill marks in Fig. 5 (number of profiles in each section is 56, 56 and 44). The water entering the channel from Marguerite Trough shows the largest variation on an isopycnal, with standard deviations of potential temperatures of 0.33 ± 0.15 °C across the isopycnal layers shown. This reduces to 0.007 ± 0.002 °C after the first three sills and 0.005 ± 0.004 °C in Laubeuf Fjord, where variability shallower than 200 m increases very slightly.

The small scale variability of temperature along isopycnals is indicative of mesoscale-induced eddy filamentation with density-compensating variation in temperature and salinity (Garabato *et al.*, 2011). This variance is ultimately destroyed by both diapycnal and isopycnal mixing processes, hence the reduction in variability with distance onshore. This suggests that each of the ridges is strongly associated with vigorous horizontal or vertical mixing.

The pattern of the changes shows some agreement with the locations of deep overflows, but there are also indications of changes occurring along the entire channel. Both areas are likely to be the source of significant mixing, either by plume entrainment in the overflows or by breaking of internal waves formed where the flow interacts with rough bottom topography or from the overflows themselves, which could propagate away from the sills before breaking.

3.6 Separation of profiles above sill depth

There is an indication along the channel that temperature and salinity profiles diverge considerably above the depths of the sills. To test this, profiles are compared from inside and just outside Ryder Bay. The bathymetry here is well known through multibeam swath surveys, with the sill depth being 355 m. Figure 6 shows salinity profiles and the deep θ/S from within Ryder Bay and just outside, from two contrasting years collected with the assistance of the ARSV *Laurence M Gould*. It is clear that the profiles diverge at about 275 m, well above the sill depth. As the θ/S profiles are already straight it is hard to distinguish between mixing and stretching of profiles, though the smoothing of the θ/S in 2008 suggests mixing. Along with the θ/S changes noted above, this shows that the effect of the sills extends above their depth, through entrainment of overlying water and the stretching of profiles as water descends.

3.7 Extreme cases

A depression near the southern end of Adelaide Island, with a sill depth of approximately 150 m, was sampled with a glider in January 2013 and on the JR307 cruise in January 2015. The sill depth is too shallow to allow mCDW into the depression (Fig. 7a), instead colder pycnocline water (a mixture of mCDW and surface water) floods the depression down to its depth of just over 600 m. This water normally occupies the 100-150 m layer of the water column, but within the depression this is stretched down to the seafloor, thereby reducing the stratification considerably. The temperature at 500 m was -0.11 °C in 2013 in the depression, whereas the temperature at this depth outside the depression is 1.2 °C (Fig 7c). The θ/S properties of the water at the bottom of the depression match the properties found at about 135 m in the fjord. In 2015 the temperature inside was 0.29 °C, the increase in temperature being consistent with a shallower thermocline in this year, and is matched by an increase in salinity (Fig. 7d). The increase in salinity, and therefore density, at the bottom shows that a new overflow of water must have happened between the two sampling events as clearly vertical mixing within the depression can not cause such an effect.

A second cold hole to the west was sampled during the cruise, with two sections having deep temperatures of 0.05°C and -0.2 °C (Fig. 7c), the second seemingly being flooded by an overflow from the first. The θ/S properties (Fig. 7b) show differences between the two depressions. Despite the close proximity of the two depressions, they are separated by a very shallow ridge and are flooded from different directions. The westerly hole has T/S properties similar to the Marguerite Bay source water whereas the initial easterly hole matches the properties of water that has flown along the channel to Laubeuf Fjord and then north-west into the depression, especially so in 2015. This water has been heavily mixed on route as described above.

Similar to the early overflows along the channel described above, the deep waters in Palmer Deep (Fig. 8a) are warmer than the source water at the same depth (Fig. 8c). This again must be due to the overspilling and mixing of warm water from close to the temperature maximum as it crosses the shelf. The profiles diverge considerably above the sill depth of approximately 500 m (Fig. 8d). The θ/S relationships also change considerably, with considerably different WW endmembers with distance across the shelf (Fig. 8b).

3.8 Downward propagation of surface variability

The variability in the eastern cold hole between 2013 and 2015 (Fig. 7) demonstrates that surface-driven variability can propagate to depth. Although the other sills studied are considerably deeper, there is evidence of associated mixing extending shallower than 200 m and therefore there is still the likelihood of the overflows connecting surface processes to depth.

Each January a CTD cast is carried out with the RATS CTD in Laubeuf Fjord, with assistance of the ARSV *Laurence M Gould*. These casts, together with casts from the same day within Ryder Bay, allow for a study of the effects of varying winter mixing through the time series. Outside Ryder Bay there is considerable interannual variability in the WW and deep water properties (Fig. 9a,b), which feeds through to variations at depth within Ryder Bay, with the signal enhanced by the overflow and entrainment over the 355 m sill (Fig. 9c). The time series of deep temperatures (Fig. 8d) shows both seasonal variability and interannual changes. The reduction in temperature in 2008 is related to a widespread reduction in winter sea ice south of Adelaide Island in winter 2007, which had persistent impacts on data recovered at the RATS site (Venables and Meredith, 2014).

Given the density-driven nature of the overflows, variability towards increased density in the source waters, such as in the eastern cold hole, are likely to propagate downwards more rapidly but the changes seen at depth in Ryder Bay between 2007 and 2008 (Figure 9) show that changes towards less dense water within the basin can also happen rapidly, suggesting a low residence time and significant vertical mixing.

4 Discussion

The intrusion and upwelling/mixing of deep water on the WAP shelf supplies heat to both the atmosphere and cryosphere, and understanding the details of this heat flux is therefore crucial for increasing predictive skill concerning future changes in the region. This study highlights the importance of interactions with bathymetry. The localised nature of the mixing associated with the overflows highlights specific areas that we suggest should be target sites for future detailed process studies, including direct quantification of turbulence. The localised nature also poses an additional challenge to numerical simulations of the region, as it requires the inclusion of small-scale processes and realistic bathymetry that are imperfectly known and challenging to represent in models. The strong dependence on local bathymetry also means that obtaining a purely observational estimate of the heat flux onto the shelf would require a careful and prolonged measurement of every pathway by which water accesses or leaves the shelf (the heat flux being related to the temperature difference between the two), in addition to determination of heat loss to the atmosphere.

It is clear from this study that, given a suitable bathymetric configuration, remarkably strong links between surface variability and deep temperatures can exist. Given the changes in sea ice observed across wide regions of Antarctica (Holland and Kwok, 2012; Stammerjohn *et al.*, 2008b) and the high level of surface ocean variability that can ensue in winter and the following summer (Venables and Meredith, 2014), this can potentially affect the amount of heat available for melting glacial ice at any depth. Mooring data show wintertime cooling extending to 150 m at a number of locations across the shelf (Moffat *et al.*, 2005), which may then propagate to depth through mixing and overflows. The rapid nature of these cooling events suggest they are linked to local variability in sea ice, suggesting that wider trends in ice cover will significantly affect the wintertime heat loss to the atmosphere. This will have the tendency to reduce the amount of heat available for melting ice, but changes in wind stress and density structure could affect the currents, either enhancing or counteracting this effect.

The cold depressions described here, together with the mechanisms behind the source of Palmer Deep water (and the early basins along the channel) indicate that bottom temperatures along the Antarctic Peninsula are more variable for a given depth than previously considered, and may also be subject to greater seasonal and interannual variability in some locations. These temperatures are important for benthic organisms (Clarke *et al.*, 2009) so an understanding of where the bottom temperatures may differ from the norm could improve the ability to explain current knowledge of benthic distributions (Griffiths *et al.*, 2013; Smith *et al.*, 2012) and point to priority areas for further biogeographical sampling (Kaiser *et al.*, 2013). Similarly, sediments in enclosed depressions tend to be less disturbed by near-bottom currents than outside them, and hence they can be excellent sites for the collection of sediment cores for paleo-oceanographic studies. However, interpretation of such cores (particularly with respect to any benthic organisms (Ishman and Sperling, 2002)) must take into account the depth and time variability of the source waters, which may change with varying local sea level or thermocline depth. The interpretation and regional relevance of such changes clearly requires an understanding of the controls, and we have demonstrated here that localised mixing and overflows, and thermal isolation on very small scales, can dominate the properties encountered along the WAP.

The propagation of surface variability to depth also has implications for measuring long-term ocean temperature trends. A consequence of this vertical propagation is that some areas will potentially show greater inherent variability and seasonal cycles, and will therefore be more challenging as areas from which climatic records can be constructed. There is little long-term year-round data at depth on the WAP shelf, and such data as do exist are often obtained close to the coast where such variability is strongest (Venables and Meredith, 2014). Sustained offshore observations, especially in winter, through a combination of moorings, under-ice floats, gliders and other emerging technologies, are therefore a key priority for progressing our understanding of trends on the WAP shelf.

Acknowledgements

We would like to thank Ben Allsup and Lauren Cooney from Teledyne Webb for assisting with glider operations and improving performance around ice together with David White, Alvaro Lorenzo Lopez and Sam Ward from National Oceanography Centre. Also the captain and crew of the RRS *James Clark Ross* and ARSV *Laurence M. Gould* for sampling in Marguerite Bay and glider recoveries and the Marine Assistants that have wintered at Rothera and continued the Rothera Time Series. Peter Fretwell assisted with bathymetry during and after glider deployments was also much appreciated. This paper is a contribution of the BAS Polar Oceans programme, funded by the Natural Environment Research Council.

References

Arndt, J.E., Schenke, H.W., Jakobsson, M., Nitsche, F.O., Buys, G., Goleby, B., Rebesco, M., Bohoyo, F., Hong, J., Black, J., Greku, R., Udintsev, G., Barrios, F., Reynoso-Peralta, W., Taisei, M., Wigley, R., 2013. The International Bathymetric Chart of the Southern Ocean (IBCSO) Version 1.0-A new bathymetric compilation covering circum-Antarctic waters. Geophysical Research Letters 40 (12), 3111-3117.

Bolmer, S.T., Beardsley, R.C., Pudsey, C.J., Morris, P., Wiebe, P., Hofmann, E.E., Anderson, J., Maldonado, A., 2004. A high-resolution bathymetry map for the Marguerite Bay and adjacent west Antarctic Peninsula shelf for the Southern Ocean GLOBEC Program. WHOI Technical Report.

Clarke, A., Griffiths, H.J., Barnes, D.K.A., Meredith, M.P., Grant, S.M., 2009. Spatial variation in seabed temperatures in the Southern Ocean: Implications for benthic ecology and biogeography. Journal of Geophysical Research-Biogeosciences 114.

Clarke, A., Meredith, M.P., Wallace, M.I., Brandon, M.A., Thomas, D.N., 2008. Seasonal and interannual variability in temperature, chlorophyll and macronutrients in northern Marguerite Bay, Antarctica. Deep-Sea Research Part Ii-Topical Studies in Oceanography 55 (18-19), 1988-2006.

Cook, A.J., Fox, A.J., Vaughan, D.G., Ferrigno, J.G., 2005. Retreating glacier fronts on the Antarctic Peninsula over the past half-century. Science 308 (5721), 541-544.

Garabato, A.C.N., Ferrari, R., Polzin, K.L., 2011. Eddy stirring in the Southern Ocean. Journal of Geophysical Research-Oceans 116.

Griffiths, H.J., Whittle, R.J., Roberts, S.J., Belchier, M., Linse, K., 2013. Antarctic Crabs: Invasion or Endurance? Plos One 8 (7).

Holland, P.R., Kwok, R., 2012. Wind-driven trends in Antarctic sea-ice drift. Nature Geoscience 5 (12), 872-875.

Ishman, S.E., Sperling, M.R., 2002. Benthic foraminiferal record of Holocene deep-water evolution in the Palmer Deep, western Antarctic Peninsula. Geology 30 (5), 435-438.

Kaiser, S., Brandao, S.N., Brix, S., Barnes, D.K.A., Bowden, D.A., Ingels, J., Leese, F., Schiaparelli, S., Arango, C.P., Badhe, R., Bax, N., Blazewicz-Paszkowycz, M., Brandt, A., Brenke, N., Catarino, A.I., David, B., De Ridder, C., Dubois, P., Ellingsen, K.E., Glover, A.G., Griffiths, H.J., Gutt, J., Halanych, K.M., Havermans, C., Held, C., Janussen, D., Lorz, A.N., Pearce, D.A., Pierrat, B., Riehl, T., Rose, A., Sands, C.J., Soler-Membrives, A., Schuller, M., Strugnell, J.M., Vanreusel, A., Veit-Kohler, G., Wilson, N.G., Yasuhara, M., 2013. Patterns, processes and vulnerability of Southern Ocean benthos: a decadal leap in knowledge and understanding. Marine Biology 160 (9), 2295-2317.

King, B.A., Firing, Y., 2015. RRS James Clark Ross Cruise JR306, Hydrographic measurements on WOCE line SR1b. National Oceanography Centre, Cruise Report.

Klinck, J.M., Dinniman, M.S., 2010. Exchange across the shelf break at high southern latitudes. Ocean Science 6 (2), 513-524.

Klinck, J.M., Hofmann, E.E., Beardsley, R.C., Salihoglu, B., Howard, S., 2004. Water-mass properties and circulation on the west Antarctic Peninsula Continental Shelf in Austral Fall and Winter 2001. Deep-Sea Research Part Ii-Topical Studies in Oceanography 51 (17-19), 1925-1946.

Livingstone, S.J., Cofaigh, C.O., Stokes, C.R., Hillenbrand, C.-D., Vieli, A., Jamieson, S.S.R., 2013. Glacial geomorphology of Marguerite Bay Palaeo-Ice stream, western Antarctic Peninsula. Journal of Maps 9 (4), 558-572.

Martinson, D.G., McKee, D.C., 2012. Transport of warm Upper Circumpolar Deep Water onto the western Antarctic Peninsula continental shelf. Ocean Science 8 (4), 433-442.

Martinson, D.G., Stammerjohn, S.E., Iannuzzi, R.A., Smith, R.C., Vernet, M., 2008. Western Antarctic Peninsula physical oceanography and spatio-temporal variability. Deep-Sea Research Part Ii-Topical Studies in Oceanography 55 (18-19), 1964-1987.

Meredith, M.P., Venables, H.J., Clarke, A., Ducklow, H.W., Erickson, M., Leng, M.J., Lenaerts, J.T.M., van den Broeke, M.R., 2013. The Freshwater System West of the Antarctic Peninsula: Spatial and Temporal Changes. Journal of Climate 26 (5), 1669-1684.
Moffat, C., Beardsley, R.C., Limeburner, R., Owens, B., Caruso, M., Hyatt, J., 2005. Southern Ocean GLOBEC Moored Array and Automated Weather Station Data Report. WHOI Technical Report.
Moffat, C., Beardsley, R.C., Owens, B., van Lipzig, N., 2008. A first description of the Antarctic Peninsula Coastal Current. Deep-Sea Research Part Ii-Topical Studies in Oceanography 55 (3-4), 277-293.
Moffat, C., Owens, B., Beardsley, R.C., 2009. On the characteristics of Circumpolar Deep Water intrusions to the west Antarctic Peninsula Continental Shelf. Journal of Geophysical Research-Oceans 114.
Pritchard, H.D., Arthern, R.J., Vaughan, D.G., Edwards, L.A., 2009. Extensive dynamic thinning on the margins of the Greenland and Antarctic ice sheets. Nature 461 (7266), 971-975.
Pritchard, H.D., Ligtenberg, S.R.M., Fricker, H.A., Vaughan, D.G., van den Broeke, M.R., Padman, L., 2012. Antarctic ice-sheet loss driven by basal melting of ice shelves. Nature 484 (7395), 502-505.
Rignot, E., Jacobs, S., Mouginot, J., Scheuchl, B., 2013. Ice-Shelf Melting Around Antarctica. Science 341 (6143), 266-270.
Schmidtko, S., Heywood, K.J., Thompson, A.F., Aoki, S., 2014. Multidecadal warming of Antarctic waters. Science 346 (6214), 1227-1231.
Smith, C.R., Grange, L.J., Honig, D.L., Naudts, L., Huber, B., Guidi, L., Domack, E., 2012. A large population of king crabs in Palmer Deep on the west Antarctic Peninsula shelf and potential invasive impacts. Proceedings of the Royal Society B-Biological Sciences 279 (1730), 1017-1026.
Stammerjohn, S.E., Martinson, D.G., Smith, R.C., Iannuzzi, R.A., 2008a. Sea ice in the western Antarctic Peninsula region: Spatio-temporal variability from ecological and climate change perspectives. Deep-Sea Research Part Ii-Topical Studies in Oceanography 55 (18-19), 2041-2058.
Stammerjohn, S.E., Martinson, D.G., Smith, R.C., Yuan, X., Rind, D., 2008b. Trends in Antarctic annual sea ice retreat and advance and their relation to El Nino-Southern Oscillation and Southern Annular Mode variability. Journal of Geophysical Research-Oceans 113 (C3).
Turner, J., Colwell, S.R., Marshall, G.J., Lachlan-Cope, T.A., Carleton, A.M., Jones, P.D., Lagun, V., Reid, P.A., Iagovkina, S., 2005. Antarctic climate change during the last 50 years. International Journal of Climatology 25 (3), 279-294.
Turner, J., Maksym, T., Phillips, T., Marshall, G.J., Meredith, M.P., 2013. The impact of changes in sea ice advance on the large winter warming on the western Antarctic Peninsula. International Journal of Climatology 33 (4), 852-861.
Venables, H.J., Clarke, A., Meredith, M.P., 2013. Wintertime controls on summer stratification and productivity at the western Antarctic Peninsula. Limnology and Oceanography 58 (3), 1035-1047.
Venables, H.J., Meredith, M.P., 2014. Feedbacks between ice cover, ocean stratification, and heat content in Ryder Bay, western Antarctic Peninsula. Journal of Geophysical Research-Oceans 119 (8), 5323-5336.

Figure 1. Chart of the Antarctic Peninsula showing deployment locations of Marguerite Bay and near Anvers Island.

Figure 2. Map of the main glider route (arrow slightly offset), with depths binned to 100 m intervals for clarity. The coloured marks along the arrow relate to the sills marked in Figure 5.

Figure 3. Selected profiles along the channel between Marguerite Trough (red) and Laubeuf Fjord (blue). All glider profiles are shown in the background for salinity.

Figure 4. Sections of a) Density (kg m^{-3}), with 1030.1 kg m^{-3} isopycnal in bold and b) Potential temperature (°C).

Figure 5. Potential Temperature and salinity on selected σ_{500} isopycnals (increments of 0.02 kg m^{-3} from 1030.01 to 1030.15 kg m^{-3}) along the channel from Marguerite Trough to Laubeuf Fjord. With major sills marked (those in red separating regions used for statistical analysis). The depth range spanned is from 180 m to 350-550 m (the densest isopycnals increase in depth with the overflows).

Figure 6. Selected profiles inside and outside Ryder Bay in January 2008 and 2015, data from 300 m highlighted from outside (circle) and inside (triangle) Ryder Bay sill.

Figure 7. Selected profiles in enclosed depressions south of Adelaide Island and in the source regions, sampled by a glider in January 2013 and on JR307 in January 2015. Cold Hole (E) 2013 is marked as a black dot with yellow surround for clarity.

Figure 8. Glider track and profiles across the shelf leading to Palmer Deep. (The data are comparatively low resolution since they were recovered from the glider via satellite in decimated form). All profiles are shown in the background for salinity.

Figure 9. January profiles and θ/S relationships. a) Outside Ryder Bay sill, data from 150 m highlighted, b) as (a) but zoomed and with 350 m data highlighted, c) θ/S relationships inside Ryder Bay sill for casts the same day, with 350 m data highlighted, d) time series of potential temperature within Ryder Bay at 450 m.

Fig. 1

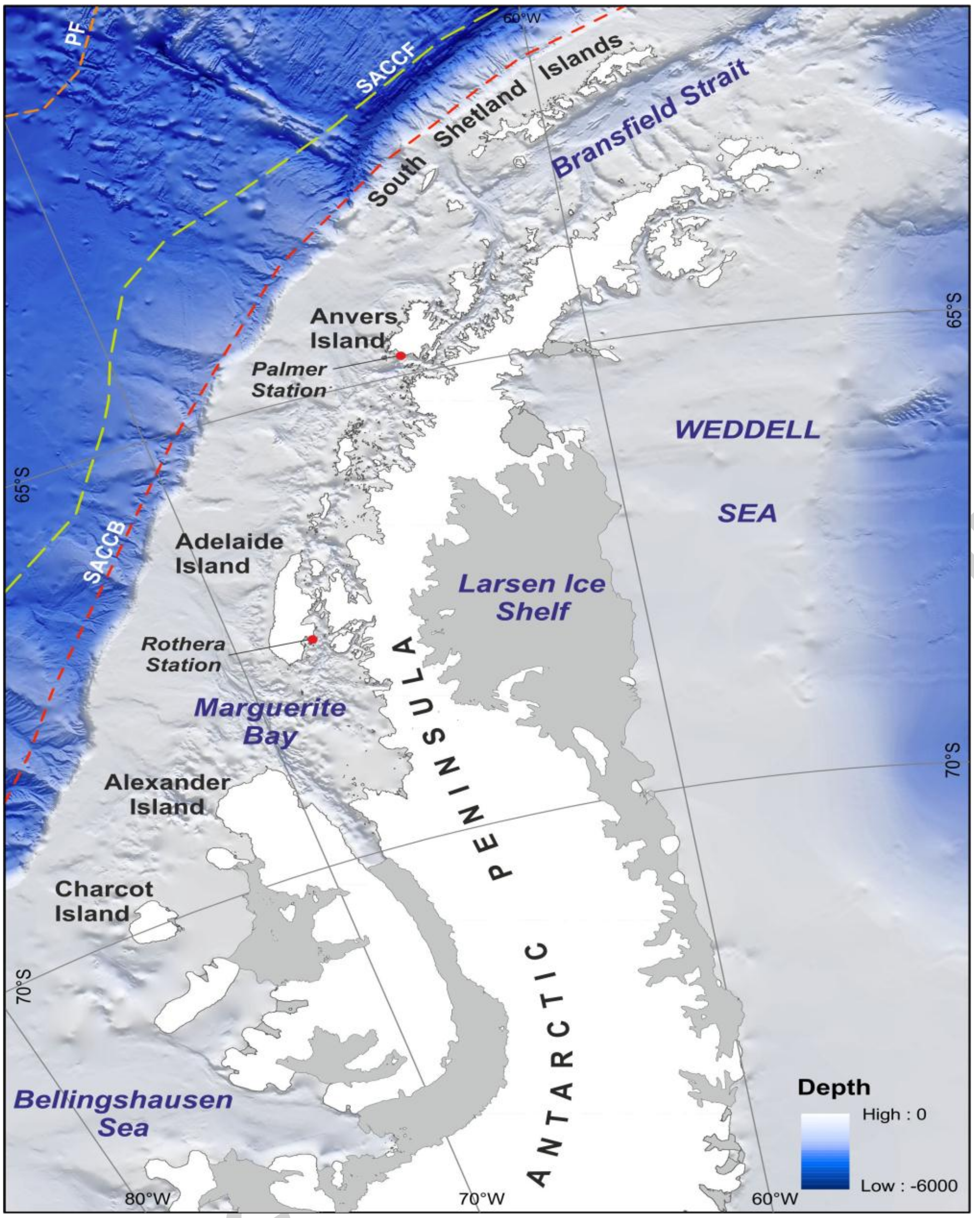
PF
SACCF
SACCB
60°W
South Shetland Islands
Bransfield Strait
Anvers Island
Palmer Station
65°S
WEDDELL SEA
Adelaide Island
Larsen Ice Shelf
Rothera Station
Marguerite Bay
70°S
Alexander Island
Charcot Island
ANTARCTIC PENINSULA
Bellingshausen Sea
Depth
High : 0
Low : -6000
80°W
70°W
60°W

Fig. 2

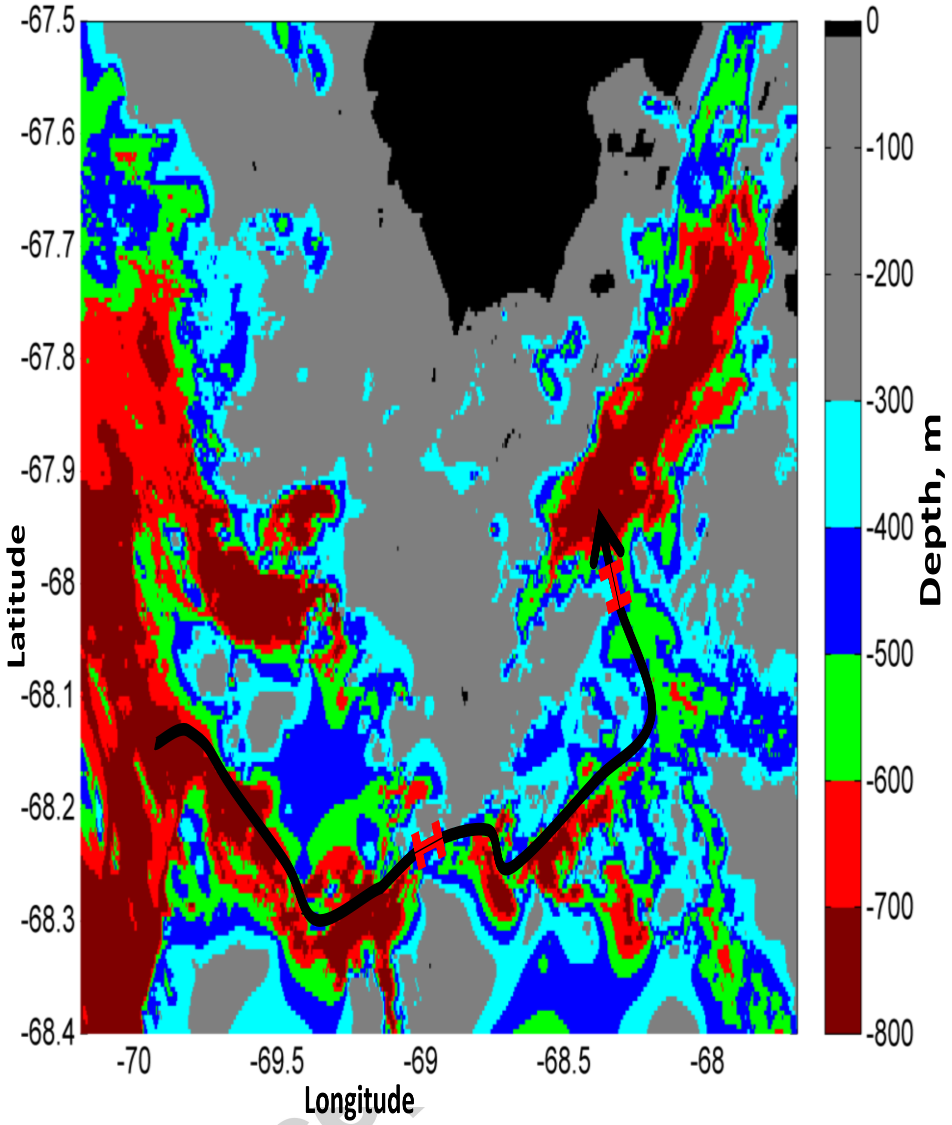
-67.5
-67.6
-67.7
-67.8
-67.9
-68
-68.1
-68.2
-68.3
-68.4
Latitude
-70
-69.5
-69
-68.5
-68
Longitude
0
-100
-200
-300
-400
-500
-600
-700
-800
Depth, m

Fig. 3

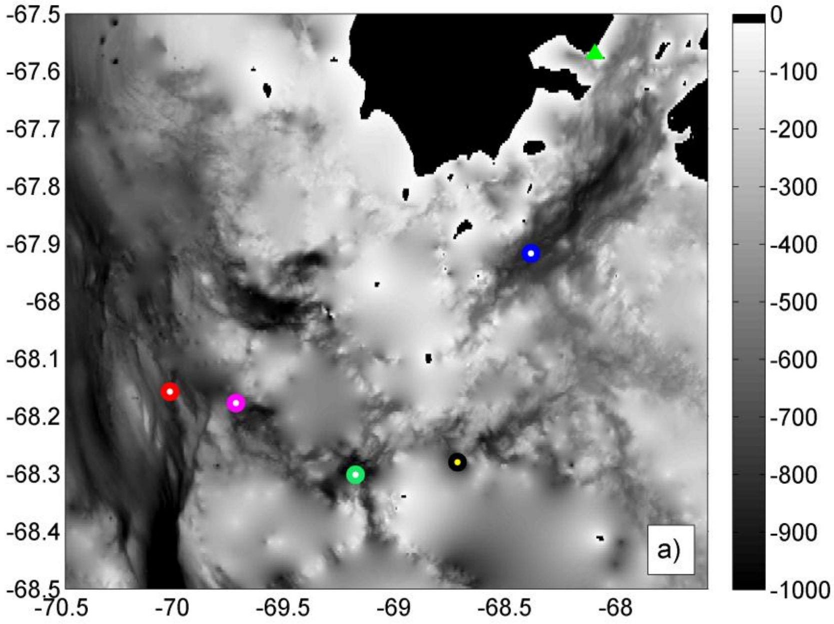
-67.5
-67.6
-67.7
-67.8
-67.9
-68
-68.1
-68.2
-68.3
-68.4
-68.5
-70.5
-70
-69.5
-69
-68.5
-68
a)
0
-100
-200
-300
-400
-500
-600
-700
-800
-900
-1000

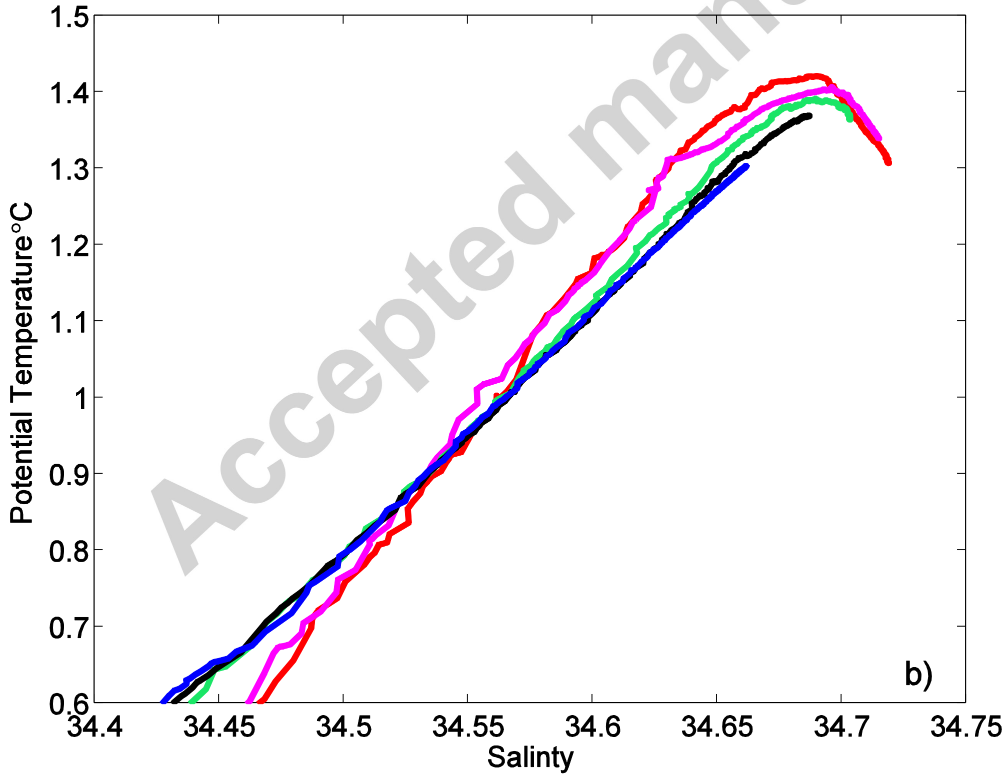
1.5
1.4
1.3
1.2
1.1
1
0.9
0.8
0.7
0.6
Potential Temperature°C
34.4
34.45
34.5
34.55
34.6
34.65
34.7
34.75
Salinty
b)

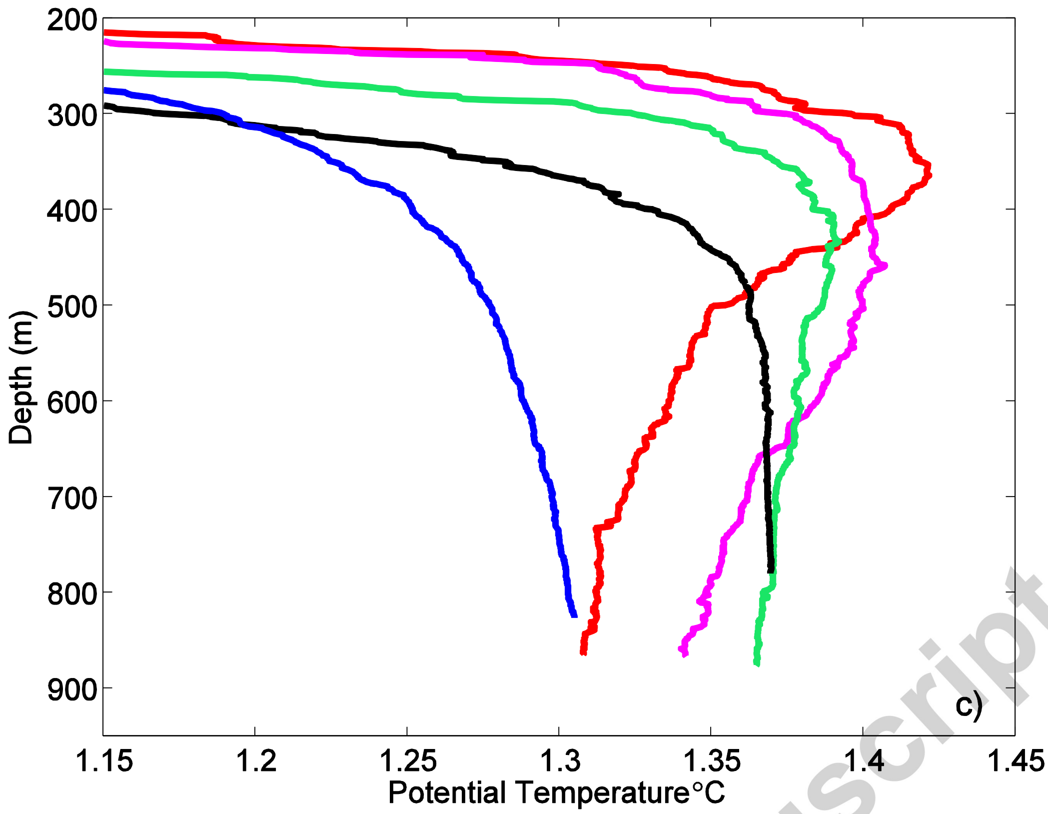
200
300
400
500
600
700
800
900
Depth (m)
1.15
1.2
1.25
1.3
1.35
1.4
1.45
Potential Temperature°C
c)

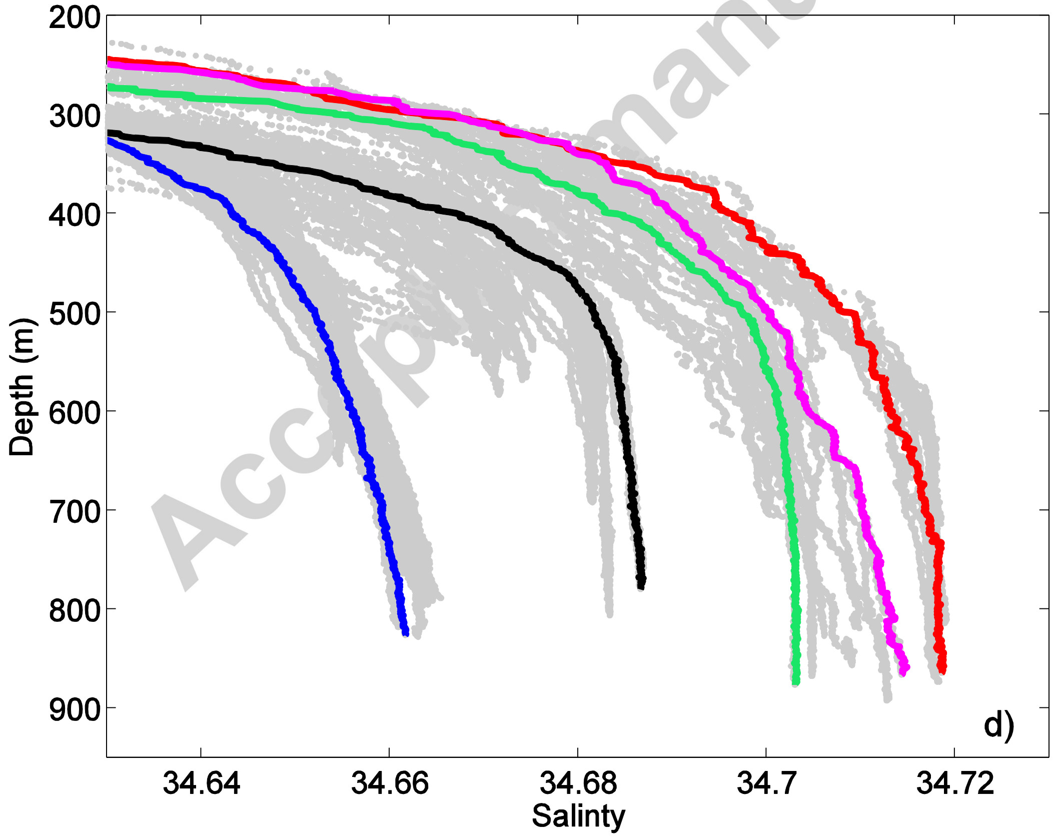
200
300
400
500
600
700
800
900
Depth (m)
34.64
34.66
34.68
34.7
34.72
Salinty
d)

Fig. 4

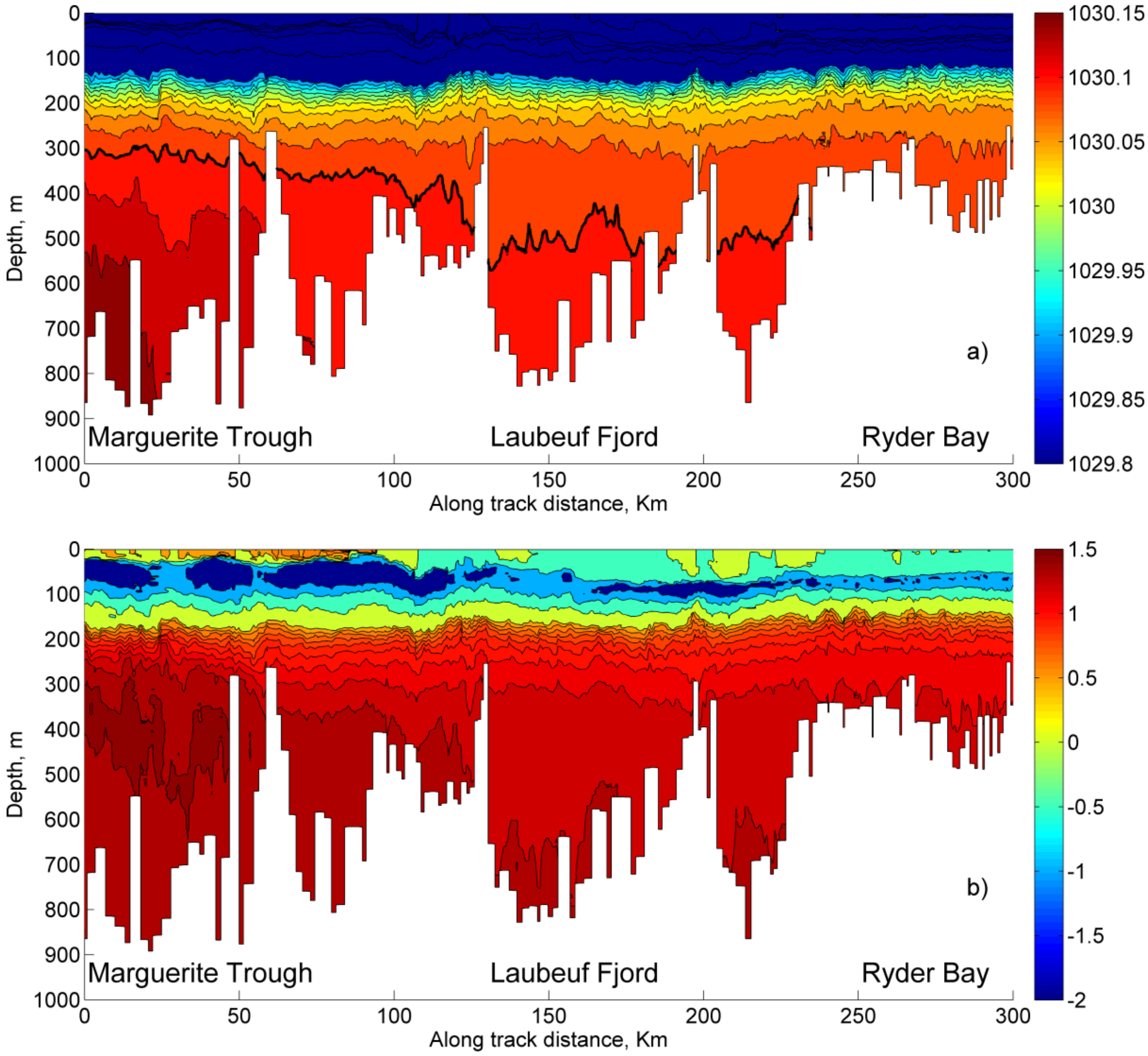

Depth, m
0
100
200
300
400
500
600
700
800
900
1000
Marguerite Trough
Laubeuf Fjord
Ryder Bay
a)
0
50
100
150
200
250
300
Along track distance, Km
1030.15
1030.1
1030.05
1030
1029.95
1029.9
1029.85
1029.8
Depth, m
Marguerite Trough
Laubeuf Fjord
Ryder Bay
b)
Along track distance, Km
1.5
1
0.5
0
-0.5
-1
-1.5
-2

Fig. 5

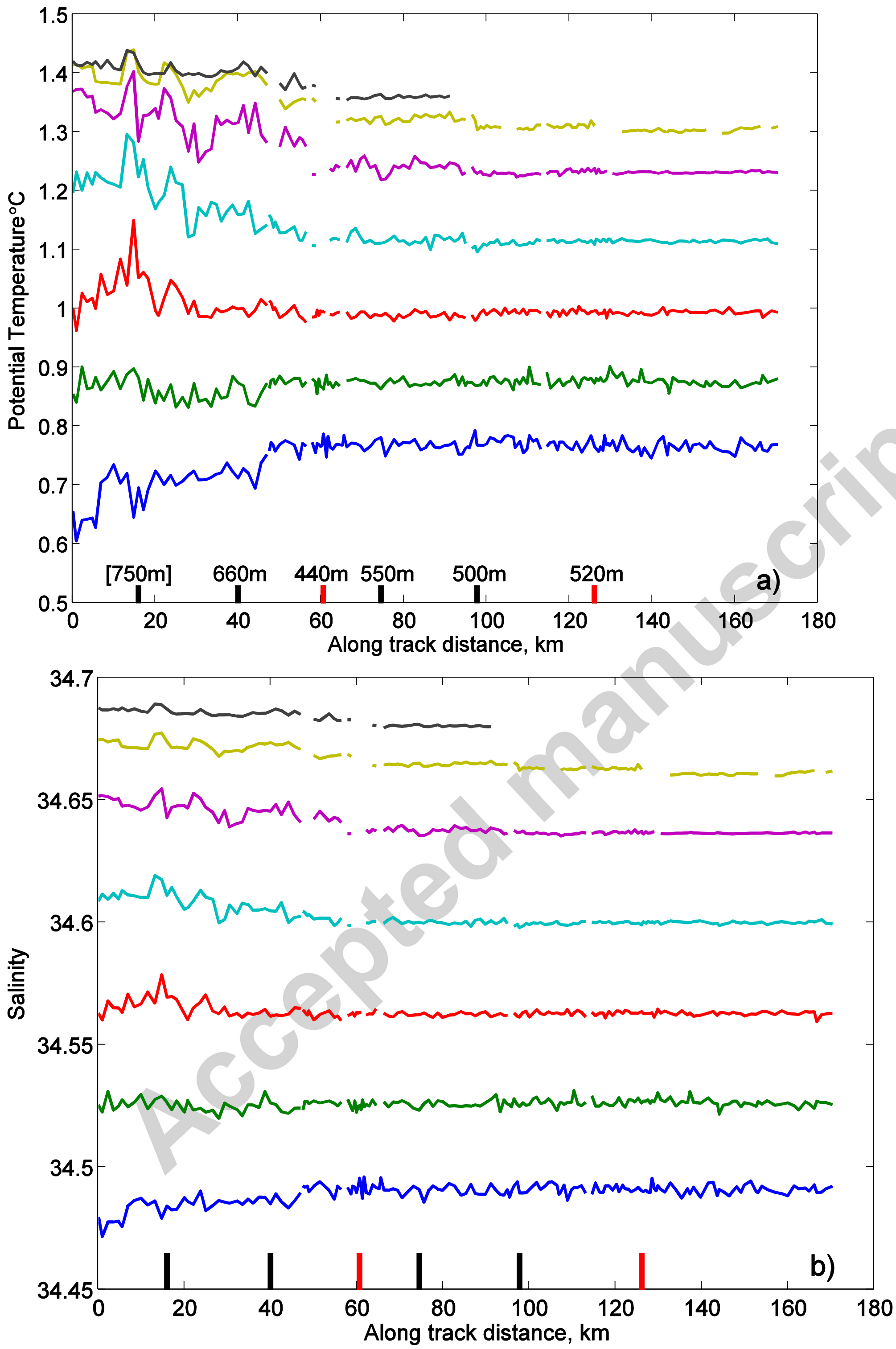

Potential Temperature°C
1.5
1.4
1.3
1.2
1.1
1
0.9
0.8
0.7
0.6
0.5
[750m]
660m
440m
550m
500m
520m
a)
0
20
40
60
80
100
120
140
160
180
Along track distance, km
Salinity
34.7
34.65
34.6
34.55
34.5
34.45
b)
Along track distance, km

Fig. 6

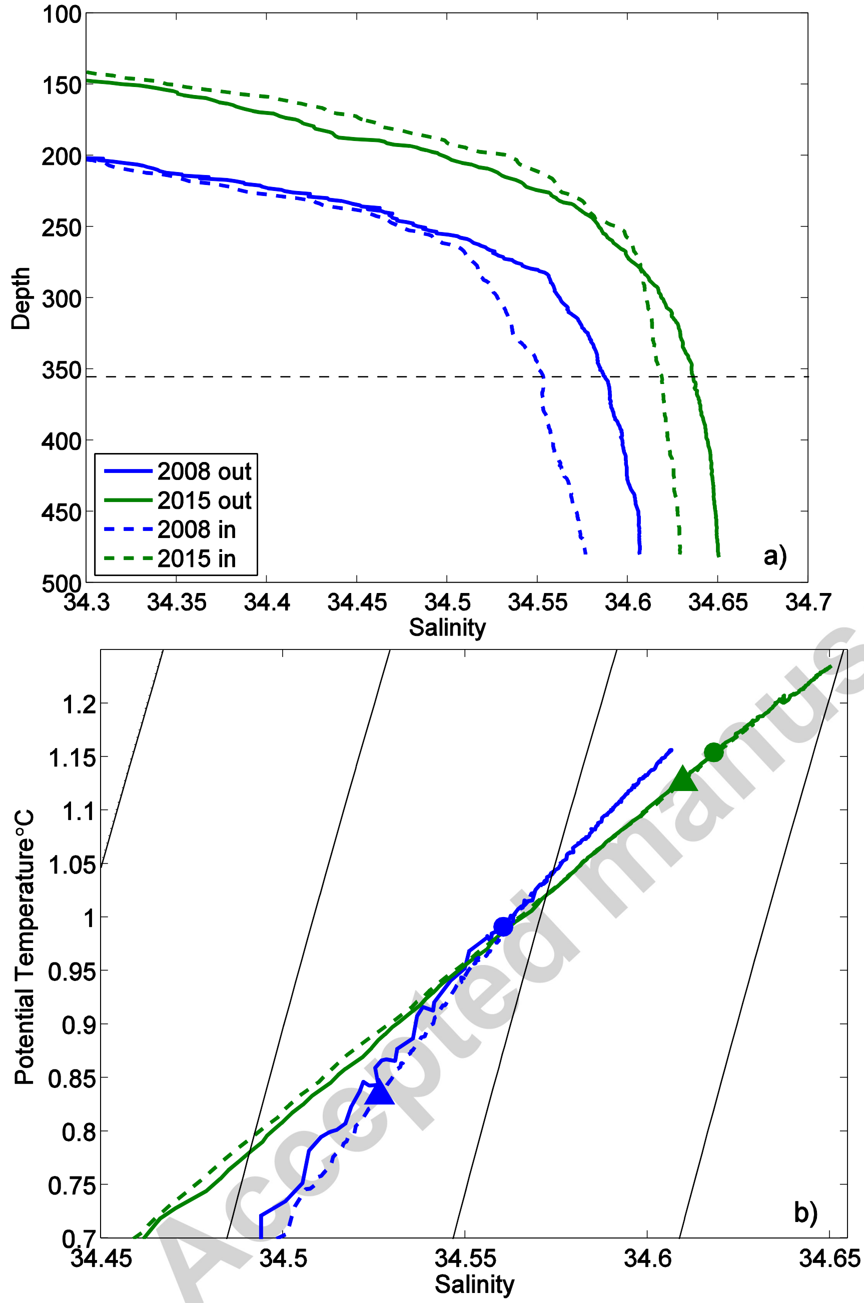

a)
Depth
Salinity
100
150
200
250
300
350
400
450
500
34.3
34.35
34.4
34.45
34.5
34.55
34.6
34.65
34.7
2008 out
2015 out
2008 in
2015 in
b)
Potential Temperature°C
Salinity
1.2
1.15
1.1
1.05
1
0.95
0.9
0.85
0.8
0.75
0.7
34.45
34.5
34.55
34.6
34.65

Fig. 7

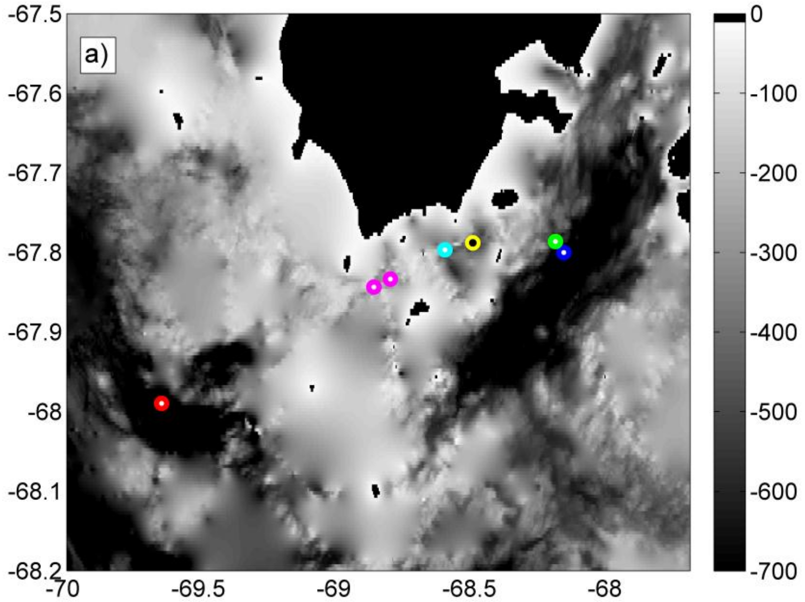
a)
-67.5
-67.6
-67.7
-67.8
-67.9
-68
-68.1
-68.2
-70
-69.5
-69
-68.5
-68
0
-100
-200
-300
-400
-500
-600
-700

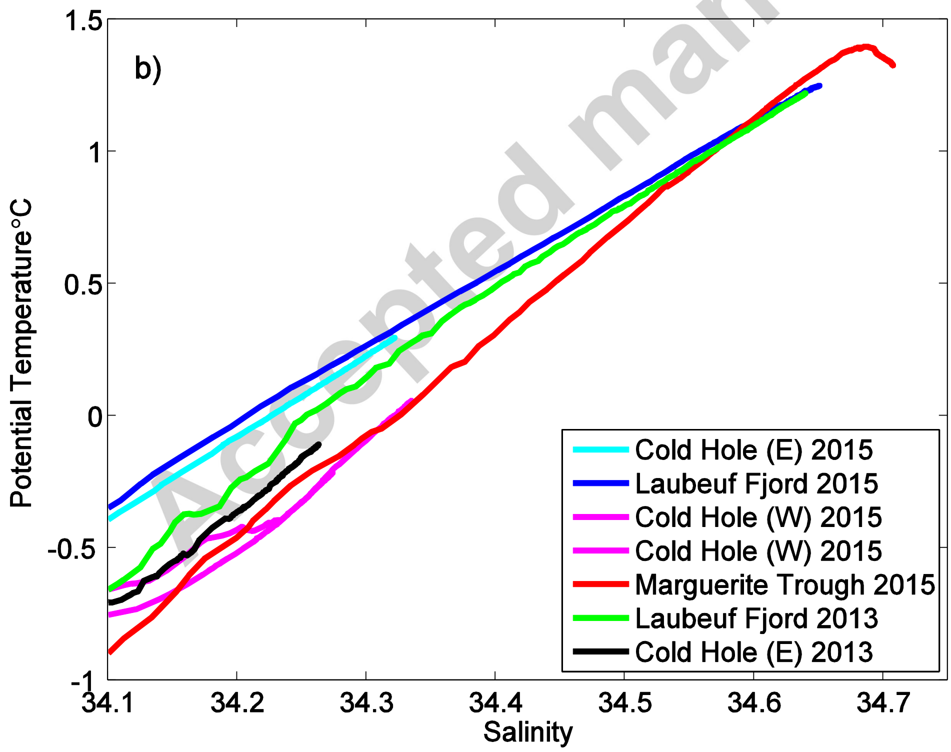
b)
Potential Temperature°C
Salinity
1.5
1
0.5
0
-0.5
-1
34.1
34.2
34.3
34.4
34.5
34.6
34.7
Cold Hole (E) 2015
Laubeuf Fjord 2015
Cold Hole (W) 2015
Cold Hole (W) 2015
Marguerite Trough 2015
Laubeuf Fjord 2013
Cold Hole (E) 2013

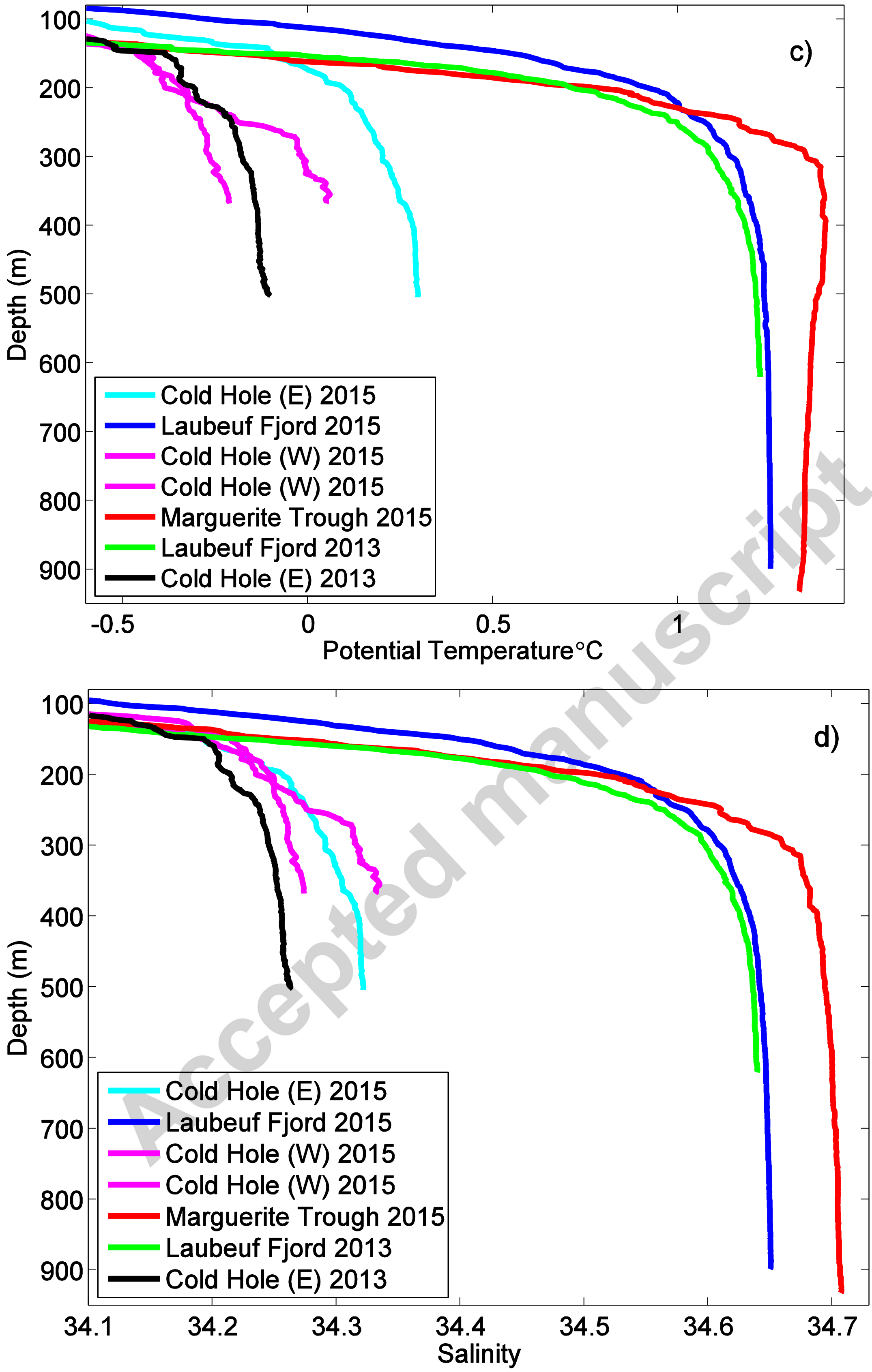
c)
Depth (m)
100
200
300
400
500
600
700
800
900
-0.5
0
0.5
1
Potential Temperature°C
Cold Hole (E) 2015
Laubeuf Fjord 2015
Cold Hole (W) 2015
Cold Hole (W) 2015
Marguerite Trough 2015
Laubeuf Fjord 2013
Cold Hole (E) 2013
d)
Depth (m)
100
200
300
400
500
600
700
800
900
34.1
34.2
34.3
34.4
34.5
34.6
34.7
Salinity
Cold Hole (E) 2015
Laubeuf Fjord 2015
Cold Hole (W) 2015
Cold Hole (W) 2015
Marguerite Trough 2015
Laubeuf Fjord 2013
Cold Hole (E) 2013

Fig. 8

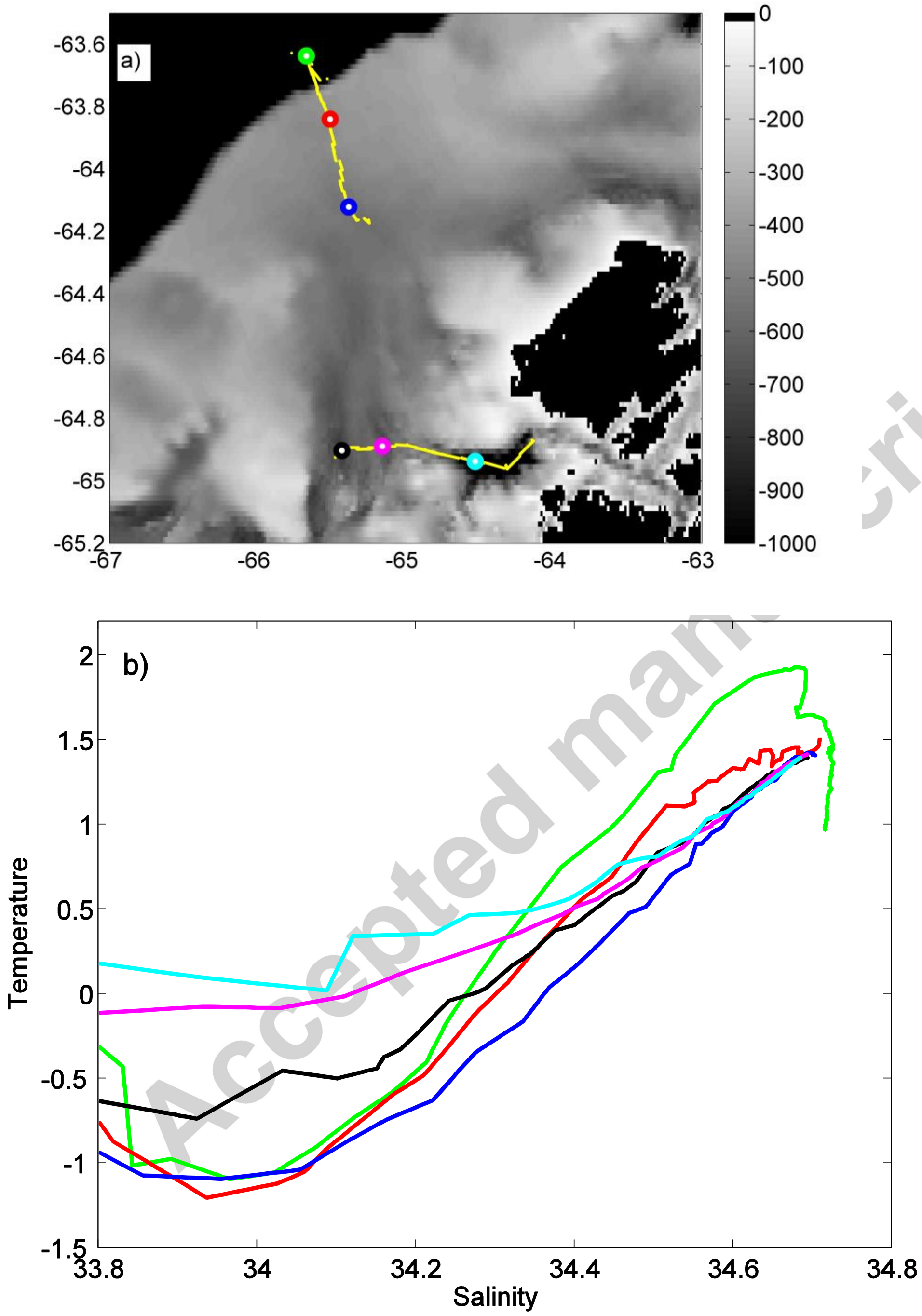
a)
-63.6
-63.8
-64
-64.2
-64.4
-64.6
-64.8
-65
-65.2
-67
-66
-65
-64
-63
0
-100
-200
-300
-400
-500
-600
-700
-800
-900
-1000
b)
Temperature
2
1.5
1
0.5
0
-0.5
-1
-1.5
33.8
34
34.2
34.4
34.6
34.8
Salinity

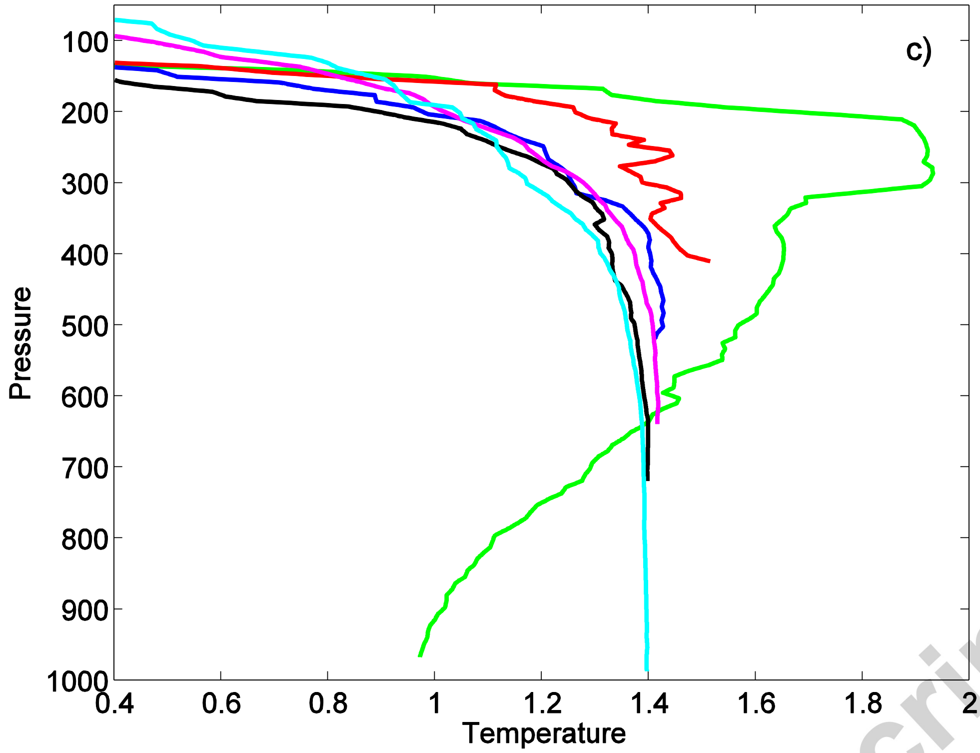

c)
Pressure
Temperature
100
200
300
400
500
600
700
800
900
1000
0.4
0.6
0.8
1
1.2
1.4
1.6
1.8
2

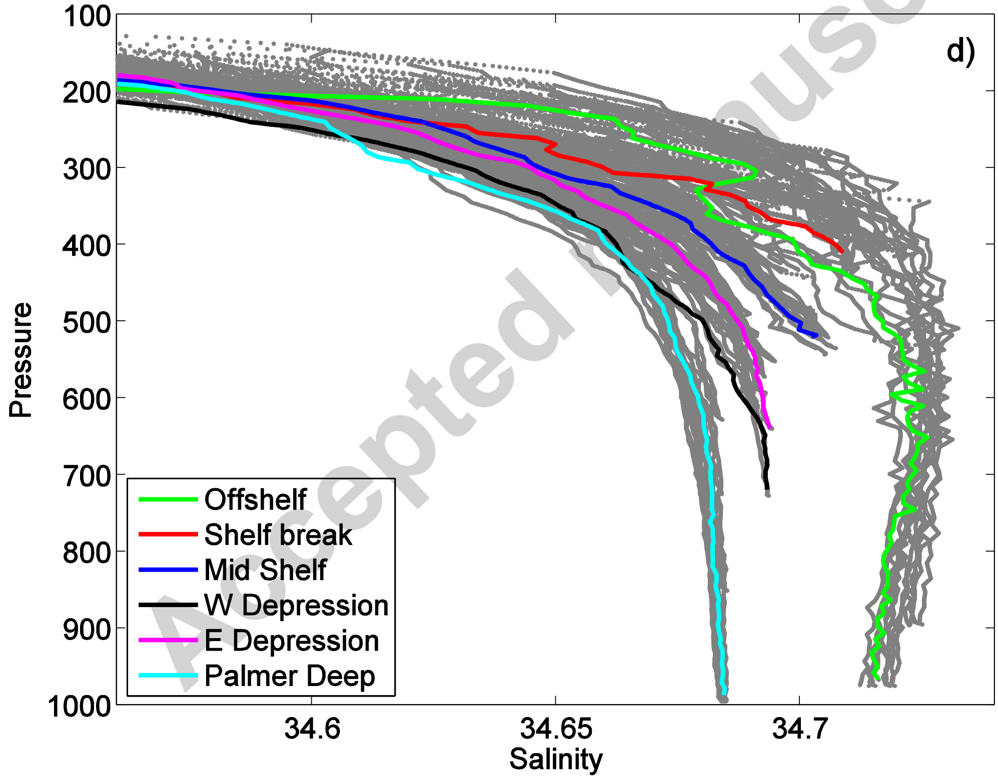

d)
Pressure
Salinity
100
200
300
400
500
600
700
800
900
1000
34.6
34.65
34.7
Offshelf
Shelf break
Mid Shelf
W Depression
E Depression
Palmer Deep

Fig. 9

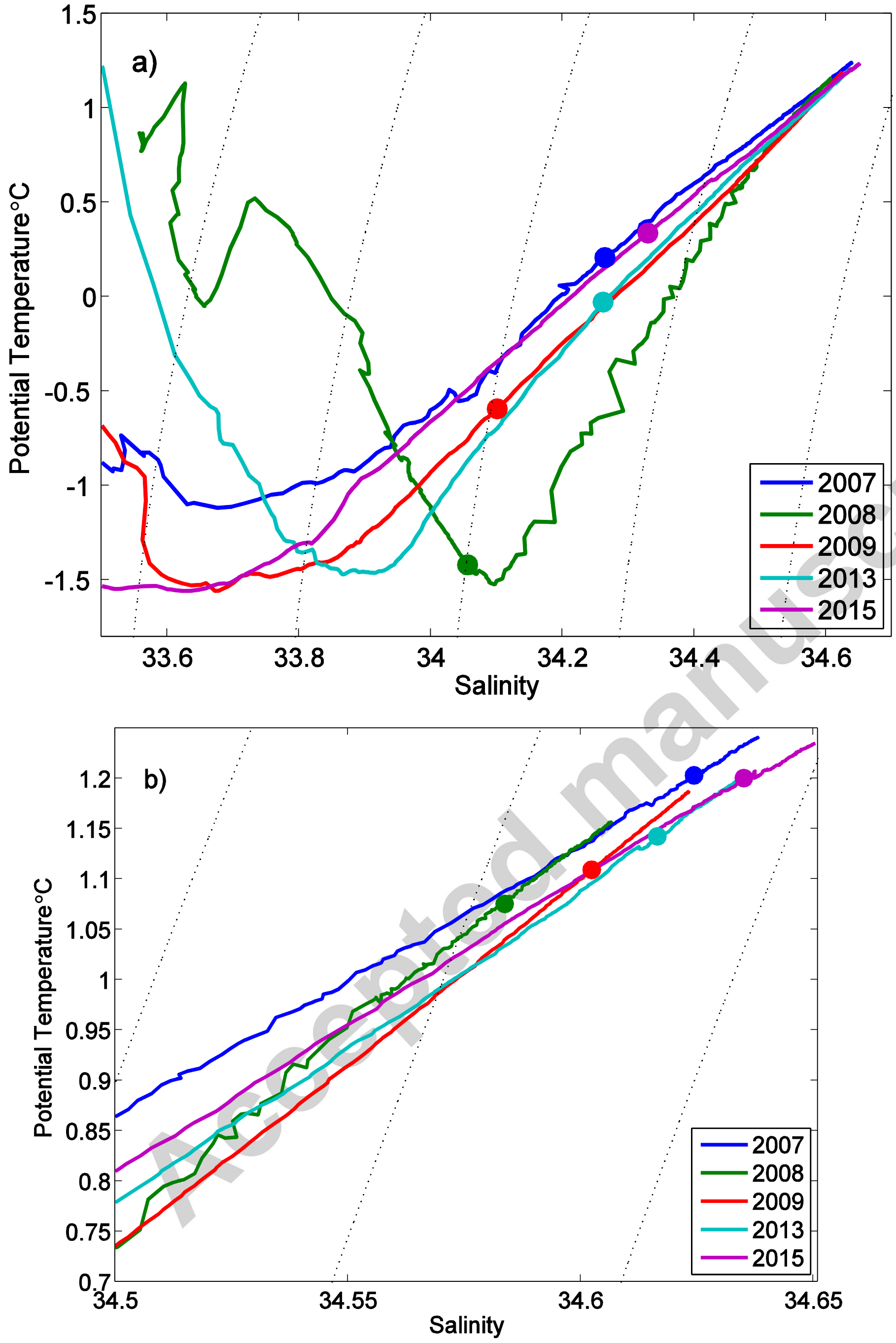
a)
1.5
1
0.5
0
-0.5
-1
-1.5
Potential Temperature°C
33.6
33.8
34
34.2
34.4
34.6
Salinity
2007
2008
2009
2013
2015
b)
1.2
1.15
1.1
1.05
1
0.95
0.9
0.85
0.8
0.75
0.7
Potential Temperature°C
34.5
34.55
34.6
34.65
Salinity
2007
2008
2009
2013
2015

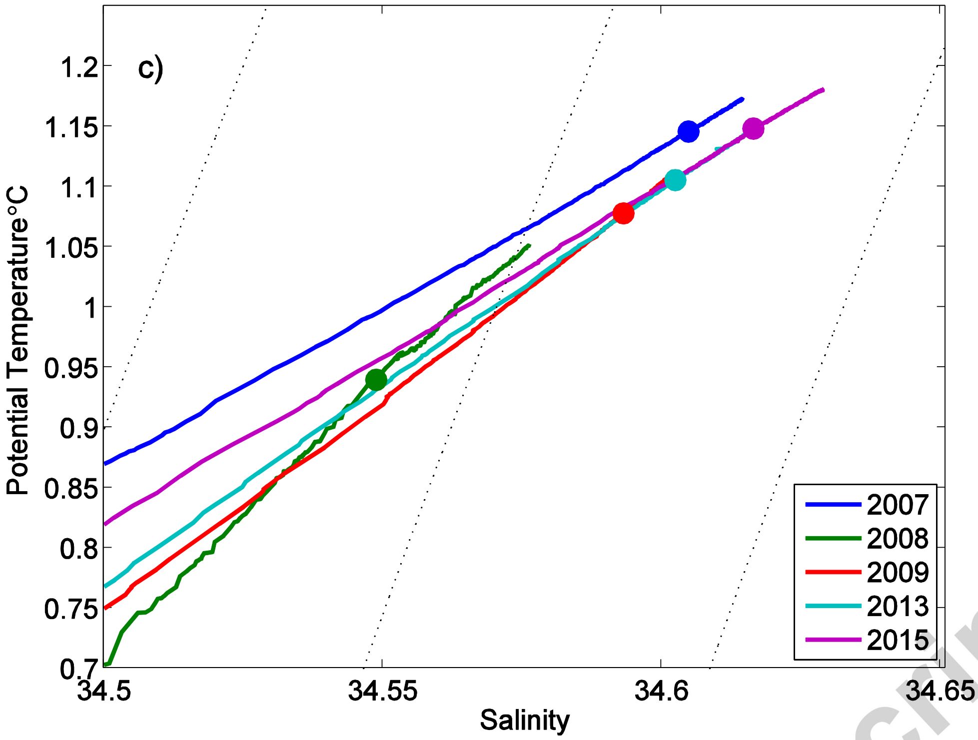
c)
Potential Temperature °C
Salinity
2007
2008
2009
2013
2015
1.2
1.15
1.1
1.05
1
0.95
0.9
0.85
0.8
0.75
0.7
34.5
34.55
34.6
34.65

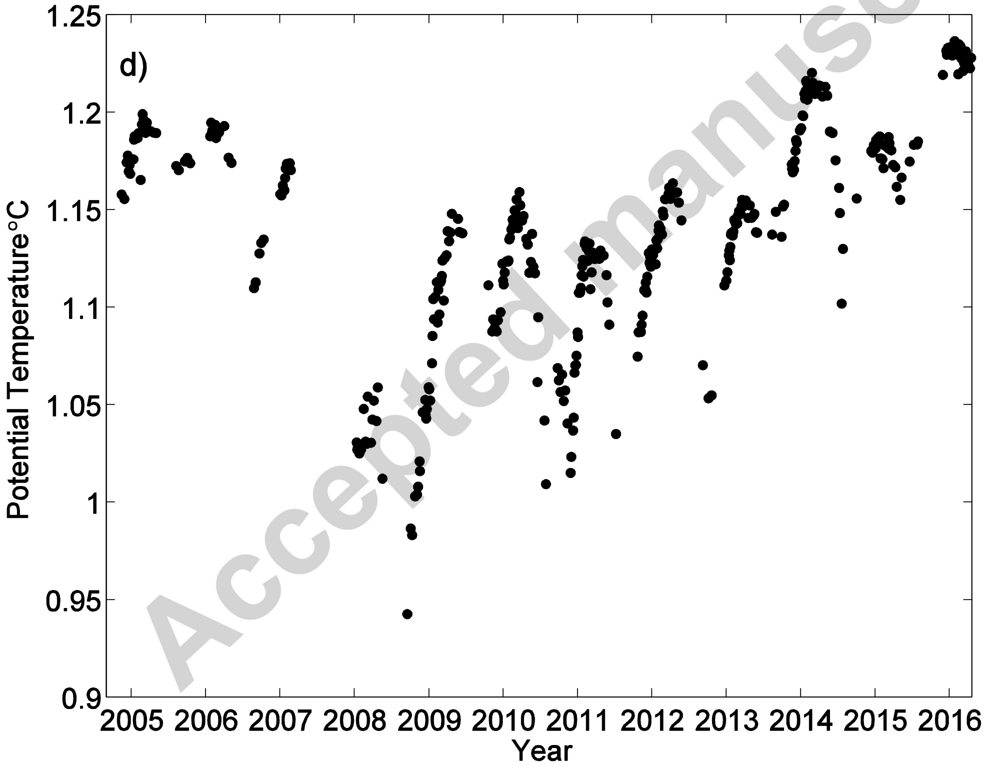
d)
Potential Temperature °C
Year
1.25
1.2
1.15
1.1
1.05
1
0.95
0.9
2005
2006
2007
2008
2009
2010
2011
2012
2013
2014
2015
2016